ChemComm

COMMUNICATION

View Article Online
View Journal | View Issue

Cite this: *Chem. Commun.*, 2023, 59, 4071

Received 4th February 2023,
Accepted 10th March 2023

DOI: 10.1039/d3cc00523b

rsc.li/chemcomm

Preparation of ultrasmall cyclodextrin nanogels by an inverse emulsion method using a cationic surfactant†

Satomi Takeuchi,[a] Andrea Cesari,[b] Suzuka Soma,[a] Yota Suzuki,[a] Maria Antonietta Casulli,[a] Kai Sato,[a] Fabrizio Mancin,[b] Takeshi Hashimoto[a] and Takashi Hayashita *[a]

Stable water-in-oil emulsion membranes can be prepared using [dilauryl(dimethyl)ammonium] bromide (DDAB), a cationic surfactant. We prepared ultrasmall cyclodextrin (γ-CyD) nanogels (γ-CyDngs) by forming ionic pairs between the secondary hydroxyl groups of γ-CyDs and DDAB. Fluorescence and NMR characterisation of the obtained γ-CyDngs revealed superior inclusion affinities compared with native γ-CyDs, beneficial for the solubilisation of hydrophobic compounds in water.

An estimated 40% of currently marketed drugs and approximately 90% of new drug candidates at therapeutic concentrations are insoluble in physiological fluids.[1] Globally, recent research has focused on developing methods for efficient drug delivery to the target site. Examples of such delivery systems include micelles, liposomes, amphiphilic nanocarriers, and nanogels.[2] Structurally, nanogels are composed of polymer chains dispersed in a large volume of liquid to form a three-dimensional network.[3] Unlike large hydrogels, nanogels have physical and chemical properties that are inherent to their nanoscale size.[4] Drug molecules can be incorporated into nanogel networks, and their release can be triggered by stimulus-responsive conformational transformation and tuned by introducing different functional groups.[5] Moreover, the large, overall surface-to-volume ratio of nanogels is advantageous because it improves the ability of nanogels to interact with target agents. In this sense, the applicability of nanogels can be extended to many other biomedical systems, from biomarker sensing[6] to the formation of functionalised coatings.[7] Recently, cyclodextrins (CyDs) have emerged as suitable building blocks for the design of advanced materials, including nanogels. CyDs are cyclic oligosaccharides composed of six (α-CyD), seven (β-CyD), or eight (γ-CyD) glucopyranose units linked by α-1,4 bonds. CyDs are shaped like a rigid torus with a hydrophobic cavity and a hydrophilic exterior surface. Thus, CyDs function as a host of supramolecular complexes by encapsulating hydrophobic molecules.[8–11] The hydroxyl groups of CyDs are highly reactive and can react with appropriate bifunctional cross-linkers to form CyD-grafted polymers having a network structure.[12,13] When CyDs are polymerised into hydrogels, their ability to form inclusion complexes in water is typically retained or even improved. Several cross-linking agents containing aldehyde, ketone, isocyanate, or epoxide groups have been reported,[14] with resulting particles having sizes in the range of tens to hundreds of nanometres.[4] Loftsson and co-workers used a water-in-oil emulsification method to control nanogel size. By adjusting the concentration of neutral surfactant Span 80 used as an emulsifier, they obtained CyD nanogels with an apparent hydrodynamic radius of 10–200 nm.[15] Unfortunately, however, nanogels of this size cannot undergo renal clearance.[16] To avoid issues of toxicity or organ/tissue accumulation, nanogels measuring up to 10 nm in diameter are strongly desired.[16]

In the present study, we prepared uniform, ultrasmall γ-CyD nanogels (**γ-CyDngs**) with ≈10 nm particle size *via* emulsion polymerisation using [dilauryl(dimethyl)]ammonium bromide (DDAB), a cationic surfactant.[17] We performed deep nuclear magnetic resonance (NMR) characterisation to obtain structural information and clarify the γ-CyD content and the affinity of the obtained **γ-CyDngs**, and found that they exhibit superior inclusion properties compared with native CyDs as confirmed by fluorescence analysis.

Ultrasmall **γ-CyDngs** were prepared using an inverse emulsion method (Scheme 1 and Chart S1, ESI†). A two-layered mixture of toluene and a basic aqueous solution containing sodium hydroxide (0.2 M), γ-CyD, and a diepoxide cross-linker [ethylene glycol diglycidyl ether (EGDE)] was sonicated to obtain a water-in-oil heterogeneous emulsion. In this emulsification process, 1-hexanol and an oil-soluble surfactant were

[a] *Department of Materials and Life Sciences, Faculty of Science and Technology, Sophia University, 7-1, Kioi-cho, Chiyoda-ku, Tokyo 102-8554, Japan. E-mail: ta-hayas@sophia.ac.jp*
[b] *Department of Chemical Sciences, University of Padova, via Marzolo 1, 35131 Padova, Italy*

† Electronic supplementary information (ESI) available: Experimental details, preparation of nanogels, characterisation data, DLS spectra, zeta potentials, fluorescence spectra, Langmuir analysis, NMR data. See DOI: https://doi.org/10.1039/d3cc00523b

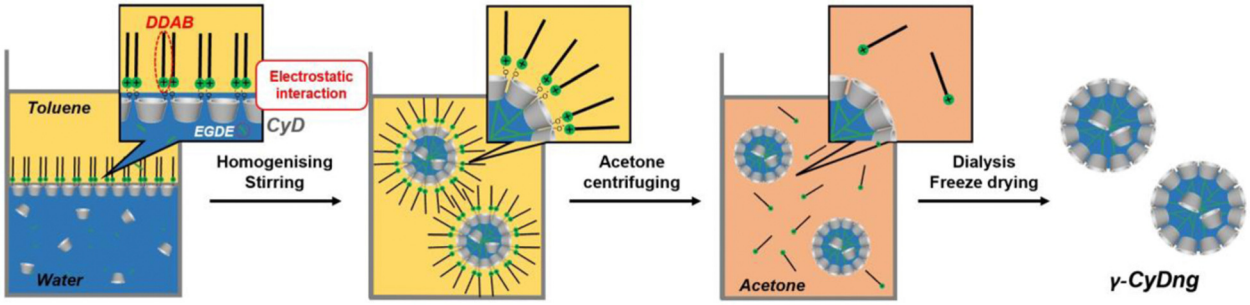

Scheme 1 Schematic illustration of the preparation of ultrasmall **γ-CyDngs**.

also added to stabilise the surface of the emulsion particles (for details, ref. to ESI†). Instead of using conventional surfactants (*e.g.*, Span 80,[15] Aerosol OT[18]), the cationic surfactant DDAB was employed in order to control the orientation of γ-CyDs, as discussed below. For the polymerisation reaction, the homogenised suspension was stirred at room temperature, and this was followed by purification of the formed nanogels by dialysis and membrane filtration. The optimal polymerisation time was set to 27 hours for the preparation of ultrasmall nanogels (the detailed explanation is mentioned in the ESI† with Table S1 and Fig. S1). Using the described protocol, spherical **γ-CyDngs** were obtained, as confirmed by transmission electron microscopy (TEM: Fig. 1 and Fig. S2, ESI†). Dynamic light scattering (DLS) measurements revealed average diameters of 4.5 ± 1.3 nm with unimodal number-size distribution (Fig. S3a, ESI†). The polydispersity index (PdI) was determined to be 0.24. These results clearly demonstrate that smaller and uniform nanogels were obtained, compared with other CyD-based nanogels previously reported.[19] Although the TEM image (Fig. 1) shows nanogels with diameters of 10–25 nm, this is reasonably consistent with the intensity-size distribution (Fig. S3b, ESI†). To characterise the dispersity of **γ-CyDngs**, the absorbance of **γ-CyDngs** at 600 nm was recorded at various concentrations. Negligible turbidity was observed in the concentration range of 5–100 mg mL^{-1} (Table S2, ESI†), showing that **γ-CyDngs** are almost transparent, *i.e.*, highly dispersed, even at high concentrations (Fig. 2a).

The polymerisation reaction performed in the absence of DDAB yielded nanogels with greatly increased PdI, suggesting a lack of uniformity in the size of the nanogels (Table S3, ESI†). This finding highlights the crucial role of DDAB in the formation of uniformly sized nanogels. Given that the secondary hydroxyl groups of γ-CyDs are deprotonated under basic condition to form O^- groups (pK_a = 12.08),[20] the anionic surface of the nanogels is likely stabilised by DDAB through electrostatic interactions (Scheme 1), thereby promoting efficient polymerisation to form nanospheres.

To examine our hypothesis that the DDAB-supported emulsion polymerisation results in the alignment of the secondary hydroxyl groups of the γ-CyD units on the nanogel surface, we performed zeta-potential measurements of **γ-CyDngs** under various pH conditions (Fig. 2b and Table S4, ESI†). Zeta potentials ranging from −0.36 ± 0.54 to −2.18 ± 1.10 mV, which were recorded between pH 3 and 11, confirmed the complete removal of DDAB. On the other hand, the negative potential observed at pH 12 (−4.12 ± 0.79 mV) suggested that the secondary hydroxyl groups were located on the nanogel surface and that they were deprotonated. As control, a nanogel consisting of only EGDE (**EGDEng**) was prepared by the same procedure as that used for **γ-CyDngs**. The zeta potentials of **EGDEng** showed no obvious shift to a negative potential at around pH 12 (Fig. S4 and Table S5, ESI†). This result clearly

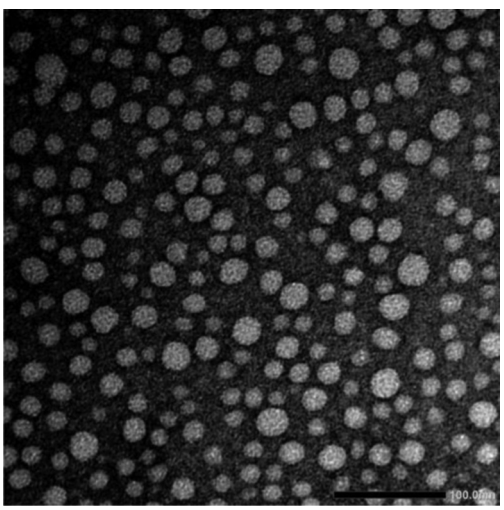

Fig. 1 TEM image of **γ-CyDngs**, scale bar: 100.0 nm.

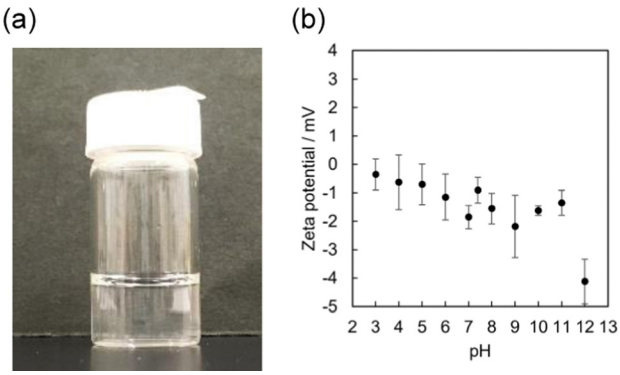

Fig. 2 (a) Image of **γ-CyDng** aqueous solution (100 mg mL^{-1}). (b) Zeta potentials of **γ-CyDngs** in water (5 mM HEPES buffer) under various pH conditions (n = 5) at 25 °C.

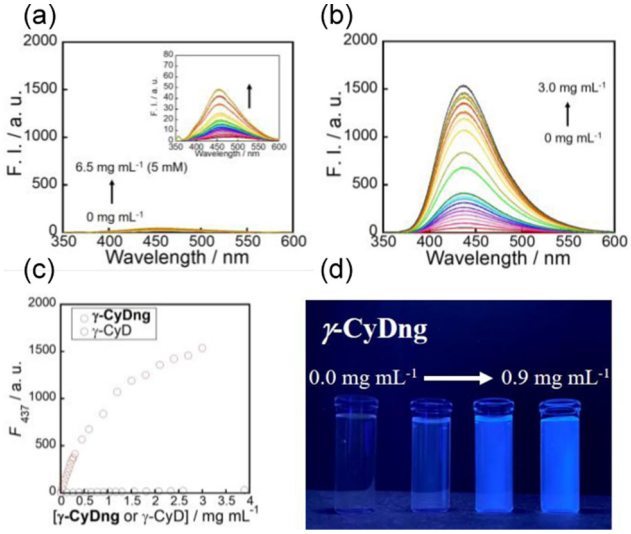

Fig. 3 Fluorescence spectra of TNS in the presence of various concentrations of γ-CyD (a) and **γ-CyDng** (b), and changes in fluorescence intensity at 437 nm (c). Measurements were performed in DMSO/water (1/99 in v/v): C_{TNS} = 10 μM, pH 7.4, 5 mM HEPES buffer, 25 °C, and λ_{ex} = 320 nm. Photograph of TNS solutions containing various concentrations of **γ-CyDng** (from left to right: 0, 0.03, 0.3, and 0.9 mg mL^{-1}) under 365 nm UV lamp irradiation (d).

supports our proposed surface structure of **γ-CyDngs**, *i.e.*, the secondary hydroxyl groups of the γ-CyD units are aligned on the nanogel surface, giving a negative zeta potential at pH 12.

To evaluate the supramolecular inclusion behaviour of **γ-CyDngs**, 6-(*p*-toluidino)-2-naphthalenesulfonate salt (TNS) was used as a guest compound. TNS can be used to evaluate the hydrophobicity of solutions as it exhibits solvent polarity-dependent fluorescence (*i.e.*, the lower the solvent polarity, the stronger the fluorescence intensity),[21] that is, the fluorescence of TNS is enhanced when it is encapsulated in the hydrophobic cavity of γ-CyD. The fluorescence intensity of TNS slightly increased with increasing native γ-CyD concentration (Fig. 3a). The association constant was determined to be 107 ± 5 M^{-1} using a one-to-one binding model (Fig. S5, ESI†). Interestingly, there was a much more dramatic enhancement in the fluorescence intensity of TNS with increasing **γ-CyDng** concentration, which was even visible to the naked eye (Fig. 3 and Fig. S6, ESI†). This clearly indicates that **γ-CyDngs** provide a more hydrophobic environment, allowing for improved inclusion of hydrophobic guest molecules, than native γ-CyDs. The affinity of **γ-CyDngs** for TNS was evaluated using the Langmuir isotherm model. The number of adsorption sites per unit gram of **γ-CyDngs** (n) and the association constant (K) were determined to be 1.90 × 10^{-4} mol g^{-1} and 3.61 × 10^{3} M^{-1}, respectively (Fig. S7 and S8, ESI†). Although the affinities of **γ-CyDngs** and native γ-CyDs are unable to be compared quantitatively since the association constants are determined based on different binding models, Fig. 3 undoubtedly demonstrates that **γ-CyDngs** exhibit much stronger fluorescent emission, indicating the superior inclusion affinity of **CyDngs** for TNS to native CyDs (the detailed explanation is mentioned in the ESI†). Unlike **γ-CyDngs**, the titration of **EGDEngs** did not show any meaningful enhancement of TNS fluorescence (Fig. S9, ESI†). The same titration measurements also indicated little or no saturation at concentrations up to 3 mg mL^{-1}. These results clearly suggest that the γ-CyD units constituting **γ-CyDngs** are responsible for the significant promotion of the adsorption of TNS, which is encapsulated in the hydrophobic γ-CyD cavities. The hydrophobicity of **γ-CyDngs** was estimated from a calibration curve relating the wavenumber of the fluorescence maximum to the solvent ratio (DMSO/H_2O), corresponding to a mixed solvent of 93% DMSO and 7% water (Fig. S10, ESI†). The results suggested the possibility of **γ-CyDngs** providing a highly hydrophobic surface, comparable to the hydrophobic environment of organic solvents, even in water, and drastically enhancing the solubility of hydrophobic compounds in water. These features are attractive from the perspective of designing nanocarrier systems for biomedical applications, such as drug delivery.

In the NMR characterisation of **γ-CyDngs**, first, we compared the ^{1}H NMR spectrum of native γ-CyDs and that of the corresponding nanogel. As shown in Fig. 4a and c, the signals from H_1–H_6 protons of γ-CyDs underwent remarkable broadening and chemical shift changes, suggesting that the assembly of supramolecular aggregates had taken place. To confirm that the observed signals were due to macromolecular and slow-diffusing species, a preliminary diffusion filter experiment was carried out. As a matter of fact, the resonances of **γ-CyDngs** in diffusion filter produced a spectral profile superimposable to the ^{1}H NMR spectrum. Thus, the formation of supramolecular aggregates was confirmed, with the incorporation of the EGDE cross-linker into the network structure. This observation made more reliable the successive NMR quantitative determination of crosslinked EGDE into **γ-CyDngs** and the quantification of γ-CyDs content, excluding the contribution of resonances produced by excess of non-bound EGDE molecules. Interestingly, signals below 3.4 ppm belonging to the EGDE cross-linker disappeared, suggesting that the molecular motions of this fragment are more quickly diffusing in solution respect to **γ-CyDngs** (more details are given further in the text). Translational diffusion coefficients (D) showed a remarkable decrease for **γ-CyDngs** [D = (0.91 ± 0.01) × 10^{-10} m^2 s^{-1}] compared with native γ-CyDs [D = (2.80 ± 0.01) × 10^{-10} m^2 s^{-1}] (Fig. S11–S13, ESI†). The hydrodynamic diameter ($d_H^{\gamma\text{-CyDng}}$ = 5.4 ± 0.2 nm,

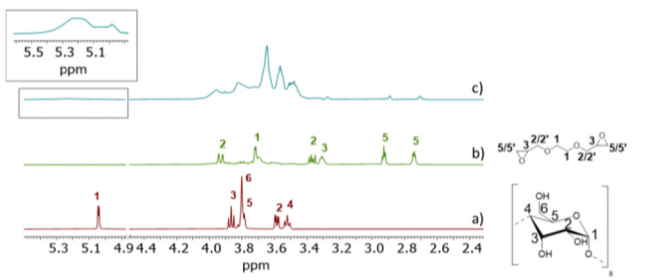

Fig. 4 ^{1}H NMR spectra (500 MHz, 25 °C, D_2O, 10 mM) of γ-CyD (a), EGDE (b), and γ-CyDng (c).

$d_H^{\gamma\text{-CyD}}$ = 1.8 ± 0.2 nm) calculated using the Stokes–Einstein equation (ref. to ESI†) for spherical molecules, as observed in TEM micrograph (Fig. 1), are in agreement with the sizes measured by DLS and those reported previously.[22] It is noteworthy that the observed anomeric proton resonance of H_1 ($H_1^{\gamma\text{-CyDng}}$) was markedly broadened by gelation relative to the resonance of the other ring protons ($H_2^{\gamma\text{-CyDng}}$ to $H_6^{\gamma\text{-CyDng}}$). This effect is attributed to the presence of a preferential orientation inside the nanogels and to the asymmetric distortion of the toroidal cone shape of native γ-CyDs. T_2 relaxation measurements (Table S6, ESI†) confirmed the increase in size of **γ-CyDngs** (average T_2 = 0.079 ± 0.001 s) relative to γ-CyDs (average T_2 = 0.216 ± 0.005 s). Slight differences in T_2 relaxation were observed between H_1 and other protons of **γ-CyDngs** (T_2 = 0.0625 ± 0.001 s and average of T_2 = 0.0956 ± 0.002 s, respectively). Finally, chemical shift changes were clearly observed in the comparison of two-dimensional heteronuclear single quantum coherence (2D HSQC) spectra between γ-CyDs and **γ-CyDngs** (Fig. S14, ESI†). The accurate acquisition of quantitative ^{1}H NMR spectra made it possible to determine the fraction of cross-linker constituting **γ-CyDngs** and γ-CyDs content in the nanogels. In the low ppm region of the ^{1}H NMR spectrum, residual signals from EGDE cross-linker protons were observed (Fig. 4b and c). These signals were broadened but had similar chemical shifts to those of the intact cross-linker. Moreover, since the average T_2 (0.12 ± 0.03 s) and D [(5.4 ± 0.5) × 10^{-11} m^2 s^{-1}] values were closer to those of a macromolecule than to those of free EGDE, the resonances at 3.27, 2.88, and 2.70 ppm could be attributed to the protons of EGDE molecules interacting with or covalently linked to **γ-CyDngs**, thus still having an epoxydic capping (Fig. 4b and c). These EGDE molecules are likely present at the ''outer'' surface and/or entrapped inside the most superficial cavities, contributing to less than 8% w/w of the total EGDE content in **γ-CyDngs**. On the other hand, excess protons resulting from doubly reacted EGDE can be calculated by removing the integral contribution of sugar ring protons, starting from $H_1^{\gamma\text{-CyDng}}$. This allows for the quantification of the γ-CyDs content (74% w/w) and the total EGDE content (26% w/w) for a single nanogel particle (Fig. S15, ESI†). These %w/w values reflect a molar ratio of about 1.9 EGDE units per γ-CyDs, confirming the high degree of intermolecular cross-linking. Finally, both the sequential additions of γ-CyDs and **γ-CyDngs** produced up-field shifts of TNS signals in the corresponding ^{1}H NMR spectra (Fig. S16 and S17, ESI†). The addition of **γ-CyDngs** broadened the ^{1}H signals of TNS due to the bigger size of nanogels receptor. These results support the fact that the disposition of available cavities make them still accessible to TNS and exposed to the solvent. In addition to that, the creation of suitable inter-CyDs space inside the nanogels can further increase **γ-CyDngs** interacting capability, as demonstrated by the higher apparent K comparison respect to native γ-CyD. In summary, **γ-CyDngs** not only retained their interacting capability but also outperformed the one of γ-CyDs.

In conclusion, we have introduced a novel method for preparing **CyDngs** *via* emulsion polymerisation using DDAB. The use of DDAB as a cationic surfactant gives control over the size of the nanogels, yielding highly uniform, ultrasmall particles ≈10 nm in diameter. We have fully characterised the so-formed nanogels through fluorescence and NMR studies, and demonstrated that these nanogels possess superior inclusion properties to native CyDs. **CyDngs** are promising candidates for biomedical applications, including the development of drug delivery systems and radiolabel markers in diagnostics.

This work was financially supported by a JSPS Grant-in-Aid for Scientific Research Grant Number 20H02772 (T. Hay.), a JSPS Research Fellowship for Young Scientists PD Grant Number 21J00709 (Y. S.) and by the Italian Association for Cancer Research (AIRC) – Investigators Grants (IG 25003). We thank Dr Yuji Tsuchido of Waseda University for helpful support in TEM and DLS measurements. We also thank Airi Okada and Yuki Iwai of Sophia University for helpful support in nanogel preparation.

Conflicts of interest

There are no conflicts to declare.

References

1 T. Loftsson and M. E. Brewster, *J. Pharm. Pharmacol.*, 2010, **62**, 1607–1621.
2 M. Suhail, J. M. Rosenholm, M. U. Minhas, S. F. Badshah, A. Naeem, K. U. Khan and M. Fahad, *Ther. Deliv.*, 2019, **10**, 697–717.
3 S. V. Vinogradov, T. K. Bronich and A. V. Kabanov, *Adv. Drug Deliv. Rev.*, 2002, **54**, 135–147.
4 M. J. Kettel, F. Dierkes, K. Schaefer, M. Moeller and A. Pich, *Polymer*, 2011, **52**, 1917–1924.
5 S. I. Sawada, Y. Sasaki, Y. Nomura and K. Akiyoshi, *Colloid Polym. Sci.*, 2011, **289**, 685–691.
6 F. Pinelli, M. Saadati, E. N. Zare, P. Makvandi, M. Masi, A. Sacchetti and F. Rossi, *Int. Mater. Rev.*, 2022, 1–25.
7 P. J. Weldrick, S. San and V. N. Paunov, *ACS Appl. Nano Mater.*, 2021, **4**, 1187–1201.
8 A. Cesari, M. A. Casulli, T. Hashimoto and T. Hayashita, *Int. J. Mol. Sci.*, 2022, **23**, 6045.
9 M. A. Casulli, I. Taurino, T. Hashimoto, S. Carrara and T. Hayashita, *ACS Appl. Bio Mater.*, 2021, **4**, 3041–3045.
10 M. A. Casulli, I. Taurino, T. Hashimoto, S. Carrara and T. Hayashita, *Small*, 2020, **16**, 2003359.
11 A. Cesari, G. Uccello Barretta, K. N. Kirschner, M. Pappalardo, L. Basile, S. Guccione, C. Russotto, M. R. Lauro, F. Cavaliere and F. Balzano, *New J. Chem.*, 2020, **44**, 16431–16441.
12 A. Cesari, A. M. Piras, Y. Zambito, G. Uccello Barretta and F. Balzano, *Int. J. Pharm.*, 2020, **587**, 119698.
13 C. Migone, L. Mattii, M. Giannasi, S. Moscato, A. Cesari, Y. Zambito and A. M. Piras, *Pharmaceutics*, 2021, **13**, 1–15.
14 C. Alvarez-Lorenzo, L. Bromberg and A. Concheiro, *Photochem. Photobiol.*, 2009, **85**, 848–860.
15 M. D. Moya-Ortega, C. Alvarez-Lorenzo, H. H. Sigurdsson, A. Concheiro and T. Loftsson, *Carbohydr. Polym.*, 2012, **87**, 2344–2351.
16 N. Licciardello, S. Hunoldt, R. Bergmann, G. Singh, C. Mamat, A. Faramus, J. L. Z. Ddungu, S. Silvestrini, M. Maggini, L. De Cola and H. Stephan, *Nanoscale*, 2018, **10**, 9880–9891.
17 T. Hayashita, R. A. Bartsch, T. Kurosawa and M. Igawa, *Anal. Chem.*, 1991, **63**, 1023–1027.
18 J. K. Oh, D. I. Lee and J. M. Park, *Prog. Polym. Sci. Oxf.*, 2009, **34**, 1261–1282.
19 M. D. Moya-Ortega, C. Alvarez-Lorenzo, A. Concheiro and T. Loftsson, *Int. J. Pharm.*, 2012, **428**, 152–163.
20 R. I. Gelb, L. M. Schwartz and D. A. Laufer, *Bioorganic Chem.*, 1982, **11**, 274–280.
21 K. Das, N. Sarkar, S. Das, K. Bhattacharyya and D. Balasubramanian, *Langmuir*, 1995, **11**, 2410–2413.
22 G. M. Pavlov, E. V. Korneeva, N. A. Smolina and U. S. Schubert, *Eur. Biophys. J.*, 2010, **39**, 371–379.

